ARTICLE NO. 79-0609aR

Helicoidal Surface Theory for Harmonic Noise of Propellers in the Far Field

Donald B. Hanson*
Hamilton Standard Div., United Technologies Corporation, Windsor Locks, Conn.

The acoustic analogy is used to derive far-field radiation equations for high-speed propellers in flight via a helicoidal surface representation of the blades. The linear thickness and loading sources and the nonlinear quadrupole sources are steady in blade-fixed coordinates. Blade sweep and offset (bending normal to the chord) appear explicitly as phase lag effects. The frequency domain results clarify the role of acoustic noncompactness, i.e., noise cancellation due to finite chord and span effects. The analysis extends, unifies, and refines the theories of several previous workers. The theory agrees well with data from a supersonic tip speed propeller.

Nomenclature

b = airfoil chord
B = number of blades
B_D = b/D, chord-to-diameter ratio
c_0 = ambient speed of sound
C_L = lift coefficient
C_D = drag coefficient
D = propeller diameter
f_i = ith component of force/unit are exerted by fluid on airfoil
FA = face alignment or offset, see Fig. 1
g = generalized source function, Eq. (15)
G = Green's function
h = thickness distribution
H = h/b, normalized thickness distribution, Fig. 3
J_n = Bessel function
k_x, k_y = wavenumbers given by Eqs. (35) and (42)
m = harmonic of blade passing frequency
MCA = midchord alignment or sweep, see Fig. 1
M_r = $\sqrt{M_x^2 + z^2 M_T^2}$ section relative Mach number
M_T = $\Omega r_T / c_0$ = tip rotational Mach number
M_x = V/c_0 = flight Mach number
n = mB = harmonic of shaft frequency
p = pressure disturbance
P_n = complex Fourier coefficient of p
$P_{Vm}, P_{Dm}, P_{11m}, P_{12m}, P_{22m}$ = see Eq. (30)
r = distance from origin to observer point
r_0 = radius of source point on blade
r_T = propeller tip radius = $D/2$
R = $|x-y|$ = distance from source point to observer
t = observer time
t_b = ratio of maximum thickness to chord
T_{ij} = quadrupole source, Eq. (2)
u = component in chordwise direction of disturbance velocity
U = $\sqrt{V^2 + \Omega^2 r_0^2}$ = local blade section speed
v = component normal to chord of disturbance velocity
V = flight speed
V_n = normal component of airfoil surface velocity
x = $(x,y,0)$ = observer coordinates
X = γ_0/b = normalized chordwise coordinate
y = observer distance from propeller axis
y_i = source coordinates y_1, y_2, y_3
Y = ξ_0/b = normalized coordinate perpendicular to chord and to radius
z = r_0/r_T = normalized radial coordinate
ξ_0 = source coordinate normal to chord (Fig. 1)
γ_i = (γ_0, ξ_0, r_0)
γ_0 = source coordinate in chordwise direction (Fig. 1)
δ_{ij} = Kroneker delta
δ = Dirac delta (impulse) function
θ = radiation angle from propeller axis to observer point
ϕ_0, ϕ_s = phase lag due to offset and sweep, Eqs. (43) and (44)
ρ = density
ρ' = disturbance density
ρ_0 = ambient density
τ = source time variable
ψ = transform of generalized source function, Eq. (19)
$\Psi_V, \Psi_D, \Psi_L, \Psi_{ij}$ = normalized source transforms, Eqs. (34), (37), (38), (41)
ω = 2π times sound frequency
Ω = 2π times shaft rotation frequency
Ω_D = $\Omega/(1 - M_x \cos\theta)$
$( )'$ = differentiation with respect to argument, as in h'

Introduction

THERE has been a renewed interest in propeller noise in recent years because of environmental concerns in general and because of the advanced turbopropellers (prop fans) being developed for fuel-conservative transport aircraft. With today's pressure to reduce noise, the designer needs to know the acoustic influence of the various design parameters at his disposal so that he can make intelligent decisions to meet weight, cost, performance, and noise requirements. The purpose of this paper is to present analytical expressions which show the mechanisms by which such parameters as thickness, chord, twist, sweep, and airfoil section shape influence noise radiation. This is accomplished via a new frequency domain analysis which displays many of the design variables explicitly.

Presented as part of Paper 79-0609 at the AIAA 5th Aeroacoustics Conference, Seattle, Wash., March 12-14, 1979; submitted May 23, 1979; revision received Dec. 27, 1979.

Index categories: Aeroacoustics; Noise; Propeller and Rotor Systems.

*Senior Analytical Engineer, Design Department, Aircraft Systems Division.

The problem to be treated is the noise of propellers in flight with uniform inflow so that all sources are steady in blade-fixed coordinates. The earliest approaches to this problem were in the frequency domain as in the works of Gutin,[1] Garrick and Watkins,[2] and Arnoldi.[3] These led to expressions for harmonic coefficients which are relatively simple except for the inevitable appearance of Bessel functions. Later, when high-speed computers became available, time domain theories, as exemplified by the works of Farassat,[4] Hanson,[5] and Schmitz and Yu,[6] were developed.These theories avoid higher transcendental functions but do require numerical differentiation and calculation of retarded blade locations. For the current application, the frequency domain was chosen because the roles of blade geometry and operating condition are much clearer. Also, the influence of acoustic "noncompactness" and how it can be used for noise reduction is more obvious in the frequency domain because blade dimensions can be compared with the wavelengths associated with harmonics of interest.

Radiation Theory

In this section, theoretical equations are derived from the acoustic analogy for later discussion. Also, comparisons with earlier propeller theory and with test data are presented.

Derivation

The starting point for the analysis is Goldstein's version of the acoustic analogy which is described as the "fundamental equation governing the generation of sound in the presence of solid boundaries" (Ref. 7, Eq. 3.6):

$$\rho'(\boldsymbol{x},t) = -\frac{1}{c_0^2}\int_{-T}^{T}\int_{S(\tau)}\left(\rho_0 V_n \frac{\partial G}{\partial \tau} + f_i \frac{\partial G}{\partial y_i}\right)\mathrm{d}S(\boldsymbol{y})\mathrm{d}\tau + \frac{1}{c_0^2}\int_{-T}^{T}\int_{\nu(\tau)} T_{ij}\frac{\partial^2 G}{\partial y_i \partial y_j}\,\mathrm{d}\boldsymbol{y}\mathrm{d}\tau \tag{1}$$

Quoting Goldstein, "it is an exact result. It applies to any region $\nu(\tau)$ which is bounded by impermeable surfaces $S(\tau)$ in arbitrary motion provided the source distributions T_{ij} and f_i are localized enough to ensure convergence of the integrals." The source terms are as follows. V_n, the normal surface velocity, will be called the monopole term in keeping with current usage despite the fact that it exhibits the characteristics of higher order poles when in motion.[7] The dipole source f_i is the ith component of the force per unit area exerted by the fluid on the boundaries. (The sign convention for V_n and f_i are opposite Goldstein's.)

The quadrupole source T_{ij} is Lighthill's stress tensor which, neglecting viscosity, is

$$T_{ij} = \rho u_i u_j + (p - c_0^2\rho')\delta_{ij} \tag{2}$$

where u_i is the ith component of the disturbance velocity in the otherwise quiescent fluid and

$$p = c_0^2\rho' \tag{3}$$

is the acoustic pressure at field points sufficiently far from the source. The integrals over the source time τ are over a range $\pm T$ large enough to include all source times of interest. For Green's function G the free space form will be used:

$$G = \frac{\delta(t-\tau-R/c_0)}{4\pi R} \tag{4}$$

where $R = |\boldsymbol{x}-\boldsymbol{y}|$ and $\boldsymbol{x}$ and $\boldsymbol{y}$ are observer and source locations measured from a reference point fixed in the quiescent fluid. For a propeller in forward flight (with one blade, for the moment), it is convenient to replace the Cartesian source coordinates with the space-fixed, locally orthogonal helicoidal coordinates $\gamma_i = (\gamma_0, \xi_0, r_0)$ defined according to

$$y_1 = \frac{\Omega r_0 \xi_0}{U} - \frac{V\gamma_0}{U}$$

$$y_2 = r_0\cos\left(\frac{V\xi_0}{r_0 U} + \frac{\Omega\gamma_0}{U}\right)$$

$$y_3 = -r_0\sin\left(\frac{V\xi_0}{r_0 U} + \frac{\Omega\gamma_0}{U}\right) \tag{5}$$

and shown in Fig. 1. The $\xi_0 = 0$ helicoid is that surface swept out by the radial pitch change axis (PCA) in forward motion at speed V and rotating at angular speed Ω. γ_0 is the distance along the helix measured from the location of the pitch change axis at $t = 0$. ξ_0 is distance normal to the helix. Both γ_0 and ξ_0 are arc lengths measured on a cylindrical surface with radius r_0. This system has the advantage over other helicoidal systems in that the γ_0 and ξ_0 coordinates also act as the conventional airfoil coordinates for an airfoil "wrapped" onto the cylindrical surface.

For an observer at $x,y,0$, the distance R is given by

$$R = \sqrt{\left(x - \frac{\Omega r_0\xi_0}{U} + \frac{V\gamma_0}{U}\right)^2 + y^2 + r_0^2 - 2yr_0\cos\left(\frac{V\xi_0}{r_0 U} + \frac{\Omega\gamma_0}{U}\right)} \tag{6}$$

In the following derivation, the approximation from thin-wing aerodynamic theory is used, permitting the surface boundary conditions to be satisfied on a mean surface rather than on the blade upper and lower surfaces. Thus, the source strengths V_n and f_i are determined from actual blade geometry but their point of action is on the mean helicoidal surface. A quantitative discussion of this approximation will be given later. For these surface sources, the surface area element becomes $\mathrm{d}S = \mathrm{d}\gamma_0\mathrm{d}r_0$. For the quadrupole source T_{ij}, which acts throughout the volume surrounding the blades, the

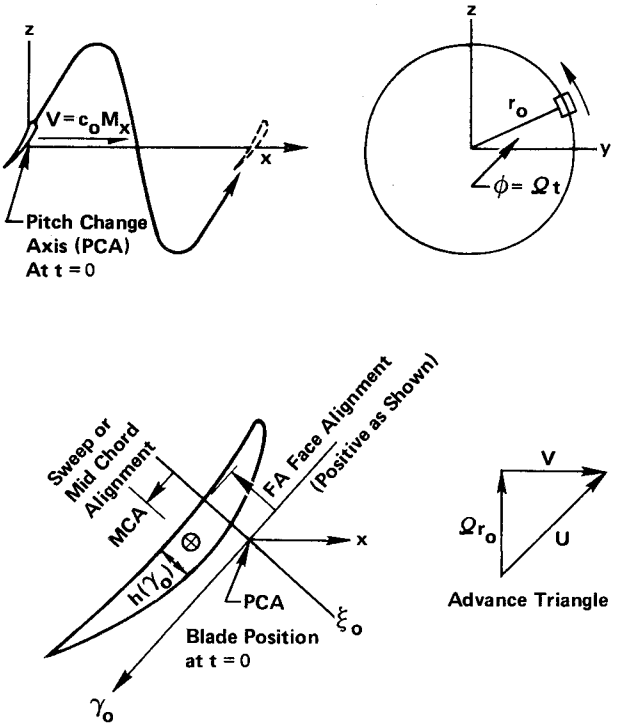

Fig. 1 Blade element shown in helical coordinates γ_0 and ξ_0.

volume element is $dy = d\xi_0 d\gamma_0 dr_0$. The volume of the blade itself is assumed to be negligible so that the volume integration is performed over all space. With these approximations the acoustic pressure becomes

$$p(x,t) = -\int_{-\infty}^{\infty}\int_0^{r_T}\int_{-\infty}^{\infty}\left(\rho_0 V_n \frac{\partial G}{\partial \tau} + f_i \frac{\partial G}{\partial \gamma_i}\right) d\gamma_0 dr_0 d\tau$$

$$+ \int_{-\infty}^{\infty}\int_0^{\infty}\int_{-\infty}^{\infty}\int T_{ij}\frac{\partial^2 G}{\partial \gamma_i \partial \gamma_j} d\xi_0 d\gamma_0 dr_0 d\tau \tag{7}$$

where T_{ij} is assumed to be sufficiently localized so that the ξ_0 integration does not extend to the helicoidal surface of the next blade. V_n and f_i are interpreted as the sum of the upper and lower surface values. For analytical convenience, the steady convected source system is replaced by an equivalent system V_n, f_i, T_{ij} that is fixed in space but timed to "turn on" in just the correct manner by the passing of the blade. Thus, the surface sources are defined for $-\infty < \gamma_0 < \infty$, but are nonzero only at the blade locations. The infinite integration range is a benefit in the Fourier transforms that follow.

Again for analytical convenience, the surface sources will be re-expressed as volume sources. The dipole source f_i at $\tau = 0$ can be written

$$f_i(\gamma_0, r_0) = \int F_i(\gamma_0, r_0, \xi_0)\, d\xi_0 \tag{8}$$

with

$$F_i(\gamma_0, r_0, \xi_0) = f_i(\gamma_0, r_0)\,\delta(\mathrm{FA} + \xi_0) \tag{9}$$

where $\delta(\mathrm{FA} + \xi_0)$ is a Dirac delta function which places the surface sources on the $\xi_0 = -\mathrm{FA}$ surface if the blade is bent or offset as shown in Fig. 1. The monopole source is given by

$$V_n = Uh'(\gamma_0, r_0) = U\int \bar{H}'(\gamma_0, r_0, \xi_0)\, d\xi_0 \tag{10}$$

where U is the local section speed

$$U = \sqrt{V^2 + \Omega^2 r_0^2} \tag{11}$$

and the local surface slope (upper and lower surfaces lumped together) is

$$h'(\gamma_0, r_0) = \frac{\partial}{\partial \gamma_0} h(\gamma_0, r_0) \tag{12}$$

Again the action at the mean surface is expressed by

$$\bar{H}(\gamma_0, r_0, \xi_0) = h(\gamma_0, r_0)\,\delta(\mathrm{FA} + \xi_0) \tag{13}$$

The only time dependance of the source considered here is that due to convention in the $-\gamma_0$ direction at speed U. Thus, if the thickness distribution $\bar{H}(\gamma_0, r_0, \xi_0)$ is as shown in Fig. 2 at time $\tau = 0$, then in general, the source distribution is given by $\bar{H}(\gamma_0 + U\tau, r_0, \xi_0)$. Thus, the acoustic pressure is given by the volume-time integral.

$$p = \int\int\int\int\Big[-\rho_0 U\bar{H}'(\gamma_0 + U\tau, r_0, \xi_0)\frac{\partial G}{\partial \tau}$$

$$- F_i(\gamma_0 + U\tau, r_0, \xi_0)\frac{\partial G}{\partial \gamma_i} + T_{ij}(\gamma_0 + U\tau, r_0, \xi_0)$$

$$\times \frac{\partial^2 G}{\partial \gamma_i \partial \gamma_j}\Big] d\xi_0 d\gamma_0 dr_0 d\tau \tag{14}$$

The partial derivatives are now moved temporarily from the Green's function onto the source functions using integration by parts. Also, a generalized source function

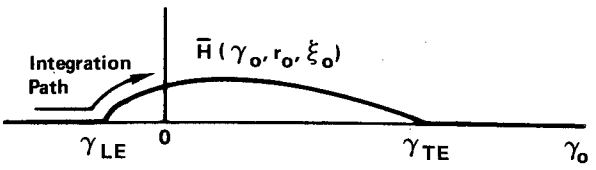

Fig. 2 Thickness source distribution at $\tau = 0$.

$$g(\gamma_0, r_0, \xi_0) = \rho_0 U^2 \bar{H}''(\gamma_0, r_0, \xi_0) + \frac{\partial}{\partial \gamma_i} F_i(\gamma_0, r_0, \xi_0)$$

$$+ \frac{\partial^2}{\partial \gamma_i \partial \gamma_j} T_{ij}(\gamma_0, r_0, \xi_0) \tag{15}$$

is defined so the pressure can be written

$$p(x,t) = \int\int\int\int g(\gamma_0 + U\tau, r_0, \xi_0)\frac{\delta(t - \tau - R/c_0)}{4\pi R} d\xi_0 d\gamma_0 dr_0 d\tau \tag{16}$$

It should be pointed out that the second derivative $\bar{H}''$ of the curve in Fig. 2 is infinite at the leading and trailing edges because the path of integration crosses the edges as shown. This could be expressed formally as a delta function $\bar{H}'(\gamma_{LE}, r_0, \xi_0)\delta(\gamma_0 - \gamma_{LE})$ at the leading edges for example; however, this turns out to be unnecessary because these derivatives are eventually removed in the chordwise Fourier transforms.

Equations (15) and (16) are equivalent to the theory derived by Morse and Ingard[8] for "radiation from a region of violent fluid motion." Since their derivation did not include any surfaces, we have demonstrated that the thin-blade approximation permits the mathematical simplification of replacing the blade surfaces by their effect on the fluid.

In Eq. (16) the τ integration may be performed first because the spatial integration limits no longer depend on τ. Thus,

$$p(x,t) = \int\int\int \frac{1}{4\pi R} g\left(\gamma_0 + Ut - \frac{UR}{c_0}, r_0, \xi_0\right) d\xi_0 d\gamma_0 dr_0 \tag{17}$$

This is essentially the formulation used previously by the author for near-field, time domain calculations.[5] Finding the values of γ_0 for which $\gamma_L \le \gamma_0 + Ut - UR/c_0 \le \gamma_T$, where γ_L and γ_T are the leading- and trailing-edge locations at $t = 0$, is the equivalent to finding the retarded location of the blade at time t.

The usual procedure for far field calculations is followed: expanding the expression for R [Eq. (6) in this case] via the binomial expansion for radiation from points near the origin to the field point r, θ. In the argument of g, terms to first order in $\gamma_0/r, \xi_0/r$, and r_0/r must be retained so that

$$R \to r - \frac{\Omega r_0}{U}\xi_0 \cos\theta + \frac{V}{U}\gamma_0 \cos\theta - r_0 \sin\theta \cos\left(\frac{V\xi_0}{Ur_0} + \frac{\Omega\gamma_0}{U}\right) \tag{18}$$

is used for retarded time calculations. For the amplitude factor $1/R$, we simply use $R \to r$.

To proceed with the derivation, a wavenumber description of the source is defined via the Fourier transform pair:

$$\psi\left(\frac{\omega}{U}, r_0, \xi_0\right) = \int_{-\infty}^{\infty} g(\gamma_0, r_0, \xi_0)\exp\left[i\frac{\omega}{U}\gamma_0\right] d\gamma_0 \tag{19}$$

$$g(\gamma_0, r_0, \xi_0) = \frac{1}{2\pi U}\int_{-\infty}^{\infty}\psi\left(\frac{\omega}{U}, r_0, \xi_0\right)\exp\left[-i\frac{\omega}{U}\gamma_0\right] d\omega \tag{20}$$

Substitution of Eq. (20) into Eq. (17) gives

$$p(x,t)=\frac{1}{8\pi^2 r}\iiint\frac{1}{U}\int\psi\left(\frac{\omega}{U},r_0,\xi_0\right)$$

$$\times\exp\left[-i\frac{\omega}{U}\left(\gamma_0+Ut-\frac{UR}{c_0}\right)\right]d\omega d\xi_0 d\gamma_0 dr_0 \tag{21}$$

But this is in the form of a Fourier integral

$$p(x,t)=\int P(x,\omega)e^{-i\omega t}d\omega \tag{22}$$

Thus, the Fourier transform of the acoustic pressure is

$$P(x,\omega)=\frac{1}{8\pi^2 r}\iiint\frac{1}{U}\psi\left(\frac{\omega}{U},r_0,\xi_0\right)$$

$$\times\exp\left[-i\frac{\omega}{U}\left(\gamma_0-\frac{UR}{c_0}\right)\right]d\xi_0 d\gamma_0 dr_0 \tag{23}$$

Substitution of Eq. (18) into Eq. (23) yields

$$P(x,\omega)=\frac{\exp\left[i\frac{\omega r_0}{c_0}\right]}{4\pi r}\iint\psi\left(\frac{\omega}{U},r_0,\xi_0\right)$$

$$\times\exp\left[-i\frac{\omega}{c_0}\frac{\Omega r_0}{U}\xi_0\cos\theta\right]I d\xi_0 dr_0 \tag{24}$$

where

$$I=\frac{1}{2\pi U}\int_{-\infty}^{\infty}\exp\left[-i\frac{\omega}{U}(1-M_x\cos\theta)\gamma_0\right]$$

$$\times\exp\left[-i\frac{\omega r_0}{c_0}\sin\theta\cos\left(\frac{\Omega\gamma_0}{U}+\frac{V\xi_0}{Ur_0}\right)\right]d\gamma_0 \tag{25}$$

and $M_x=V/c_0$ is the flight Mach number.

In the Appendix it is shown that

$$I=\frac{1}{1-M_x\cos\theta}\sum_{n=-\infty}^{\infty}J_n\left(\frac{\omega r_0}{c_0}\sin\theta\right)$$

$$\times\exp\left[in\left(\frac{V\xi_0}{Ur_0}-\frac{\pi}{2}\right)\right]\delta\left(\omega-\frac{n\Omega}{1-M_x\cos\theta}\right) \tag{26}$$

from which it follows that the noise at radiation angle θ is periodic at the Doppler frequency $(\Omega/2\pi)/(1-M_x\cos\theta)$. If we write the discrete spectrum as the sum of the harmonics

$$P(x,\omega)=\sum_{n=-\infty}^{\infty}P_n(x)\delta\left(\omega-\frac{n\Omega}{1-M_x\cos\theta}\right) \tag{27}$$

where P_n is the nth complex Fourier coefficient of the acoustic pressure, then

$$P_n(x)=\frac{\exp\left[in\left(\frac{\Omega_D r}{c_0}-\frac{\pi}{2}\right)\right]}{4\pi r(1-M_x\cos\theta)}\int_0^{\infty}J_n\left(\frac{n\Omega_D r_0}{c_0}\sin\theta\right)$$

$$\times\int_{-\infty}^{\infty}\psi\left(\frac{n\Omega_D}{U},\xi_0,r_0\right)$$

$$\times\exp\left[-i\frac{n}{U}\left(\frac{\Omega\Omega_D r_0}{c_0}\cos\theta-\frac{V}{r_0}\right)\xi_0\right]d\xi_0 dr_0 \tag{28}$$

where $\Omega_D=\Omega/(1-M_x\cos\theta)$.

This is the general far-field result for any helically convected source as given by g in Eq. (15) and its transform in Eq. (19). For B blades, the mth harmonic of blade passing frequency is found by setting $n=mB$ and multiplying by B. Waveforms can be computed from the Fourier series

$$p(t)=\sum_{m=-\infty}^{\infty}P_{mB}\exp[-imB\Omega_D t] \tag{29}$$

To study the effects of blade design parameters and operating conditions, Eq. (28) will now be recast in a form which displays these variables explicitly. Also, the noise harmonic P_{mB} will be written as the sum of several components each associated with a different source:

$$P_{mB}=P_{Vm}+P_{Dm}+P_{Lm}+P_{11m}+P_{12m}+P_{22m} \tag{30}$$

where the components are due to

P_{Vm} = volume displacement "monopole" or thickness source
P_{Dm} = drag dipole, force oriented in local convection direction
P_{Lm} = lift dipole, force oriented normal to local convection direction
P_{11m},P_{12m},P_{22m} = quadrupole components associated with the $\gamma_0,\gamma_0,\gamma_0,\xi_0$; and ξ_0,ξ_0 coordinates, respectively

The radial force and quadrupole components are ignored here but can be worked out using the techniques which follow. For the monopole term, the thickness distribution $h(\gamma_0,r_0)$ in Eq. (10) is written in terms of the shape function $H(X)$ shown in Fig. 3 with unit chord and unit thickness

$$h(\gamma_0,r_0)=bt_b H\left(X-\frac{\text{MCA}}{b}\right) \tag{31}$$

where $X=\gamma_0/b$ is the normalized chordwise coordinate; b = chord, and t_b = ratio of maximum thickness to chord. The associated wavenumber description of the thickness source from Eqs. (15) and (19) is

$$\psi_V\left(\frac{mB\Omega_D}{U},r_0,\xi_0\right)=\rho_0 U^2\int\bar{H}''(\gamma_0,r_0,\xi_0)$$

$$\times\exp\left[i\frac{mB\Omega_D}{U}\gamma_0\right]d\gamma_0 \tag{32}$$

Integration by parts, use of Eqs. (13) and (32), and an obvious change of integration variable lead to

$$\psi_V=-\rho_0 U^2 k_x^2 t_b\delta(FA+\xi_0)\exp\left[ik_x\frac{\text{MCA}}{b}\right]\Psi_V(k_x) \tag{33}$$

where

$$\Psi_V(k_x)=\int_{-1/2}^{1/2}H(X)e^{ik_x X}dX \tag{34}$$

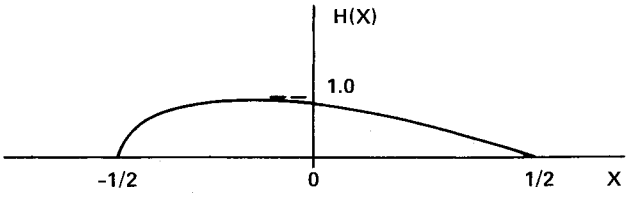

Fig. 3 Normalized thickness distribution.

and k_x is a dimensionless chordwise wave number given by

$$k_x = \frac{2mBB_D M_T}{M_r(1-M_x\cos\theta)} \tag{35}$$

Substitution of Eq. (33) and similar formulas for the other sources leads to the final result

$$\begin{Bmatrix} P_{Vm} \\ P_{Dm} \\ P_{Lm} \\ P_{11m} \\ P_{12m} \\ P_{22m} \end{Bmatrix} = -\frac{\rho_0 c_0^2 B\sin\theta \exp\left[imB\left(\frac{\Omega_D r}{c_0}-\frac{\pi}{2}\right)\right]}{8\pi\frac{y}{D}(1-M_x\cos\theta)}$$

$$\times\int M_r^2 e^{i(\phi_0+\phi_s)} J_{mB}\left(\frac{mBzM_T\sin\theta}{1-M_x\cos\theta}\right)\begin{Bmatrix} k_x^2 t_b \Psi_V(k_x) \\ ik_x(C_D/2)\Psi_D(k_x) \\ -ik_y(C_L/2)\Psi_L(k_x) \\ k_x^2\Psi_{11}(k_x,k_y) \\ 2k_xk_y\Psi_{12}(k_x,k_y) \\ k_y^2\Psi_{22}(k_x,k_y) \end{Bmatrix} dz \tag{36}$$

The radial integration limit extends to the tip for the surface sources Ψ_V, Ψ_D, and Ψ_L and to infinity for Ψ_{ij}.

The frequency domain source functions for drag and lift Ψ_D and Ψ_L are defined by equations analogous to Eq. (34):

$$\Psi_D(k_x) = \int_{-½}^{½} f_D(X) e^{ik_xX} dX \tag{37}$$

$$\Psi_L(k_x) = \int_{-½}^{½} f_L(X) e^{ik_xX} dX \tag{38}$$

where f_D and f_L are functions whose areas integrate to unity (i.e., $\Psi_D(0)=\Psi_L(0)=1$) and whose shapes express the chordwise distributions of drag and lift forces via

$$f_1(\gamma_0,r_0) = \frac{\rho_0 U^2}{2} C_D f_D\left(X-\frac{\text{MCA}}{b}\right) \tag{39}$$

$$f_2(\gamma_0,r_0) = \frac{\rho_0 U^2}{2} C_L f_L\left(X-\frac{\text{MCA}}{b}\right) \tag{40}$$

where f_1 and f_2 were discussed in conjunction with Eq.(7).

The frequency domain quadrupole source terms are

$$\Psi_{ij}(k_x,k_y) = \int\int \frac{T_{ij}}{\rho_0 U^2} e^{ik_xX} e^{ik_yY} dX dY \tag{41}$$

with T_{ij} referenced to a coordinate system fixed at the section center. Figure 4 shows the distribution of the dominant quadrupole element $T_{11}=\rho u^2+p-c_0^2\rho'$ calculated using Carlson's TRANDES computer program.[9] The source is reasonably localized around the airfoil surface.

A second wave number is defined according to

$$k_y = \frac{2mBB_D}{zM_r}\left(\frac{M_r^2\cos\theta-M_x}{1-M_x\cos\theta}\right) \tag{42}$$

The phase shifts ϕ_s and ϕ_o due to sweep and offset or face alignment, respectively, are given by

$$\phi_o = \frac{2mB}{zM_r}\left(\frac{M_r^2\cos\theta-M_x}{1-M_x\cos\theta}\right)\frac{FA}{D} \tag{43}$$

and

$$\phi_s = \frac{2mBM_T}{M_r(1-M_x\cos\theta)}\frac{\text{MCA}}{D} \tag{44}$$

General Features of the Theory

The equations above give the complex Fourier coefficients of far-field noise radiated by steady monopole, dipole, and quadrupole sources convected helically with propeller blades. They are written in terms of y, the aircraft altitude, and θ, the radiation angle. θ is a "retarded" angle, i.e., it is referred to the aircraft location when the sound was emitted. The equations contain a profusion of Doppler factors, $1/(1-M_x\cos\theta)$, in both amplitude and frequency roles. These are shown in Ref. 10 to have a strong influence at the high cruise speeds of current interest.

The dipole lift from a blade element has a two-lobe directivity pattern with the node between lobes at an angle given by $M_r^2\cos\theta-M_x=0$. The pressures in the two lobes are 180 deg out of phase and are each 90 deg out of phase with the monopole thickness noise.

Equation (36) shows that the T_{11} quadrupole radiates like the monopole term with respect to directivity and spectrum behavior. This source was discussed in detail in Ref. 11 where it was shown to be a significant contributor at transonic blade section speeds.

The limitation of the thin-blade assumption can be assessed with the aid of Eq. (44). If FA is interpreted as the error in point of application of the source in the direction normal to the chord, then ϕ_o will be the associated phase error. Consider, for simplicity, the static case, $M_x=0$, and say that the error is equal to the blade thickness bt_b. Then $\phi_0=2mBM_T B_D t_b\cos\theta$. If numbers representative of prop fans are assumed ($B=8$, $M_T=0.8$, $B_D=0.15$, $t_b=0.02$) and if ϕ_o is converted from radians to degrees, then $\phi_0=2.2\text{ deg}\times m\cos\theta$. Thus, significant phase errors occur only at very high harmonic order even near the axis. Near the plane of rotation, $\cos\theta\approx 0$, the error will be negligible at all frequencies.

Relation to Previously Published Theory

For the most part, the theory derived above is an extension of preceedings results to account for forward flight and noncompactness. The effects of offset and sweep are accounted for by phase shifts which vary with source radius. Since these have not been included explicitly in previous results, $\phi_0=\phi_s=0$ is used for the current discussion and discussion of offset and sweep is reserved for another paper.[10]

In the Arnoldi thickness noise theory,[3] a factor K appears which is the ratio of the airfoil cross-sectional area at each radius to the product of its thickness and chord. The Arnoldi theory can be recovered exactly from the first line of Eq. (36) by setting k_x in the argument of Ψ_V to zero. That is, $\Psi_V(0)$ is Arnoldi's factor K, which agrees with the definition of $\Psi_V(k_x)$ in Eq. (34). Since k_x is a measure of chordwise noncompactness, it follows that Eq. (36) is a generalization of Arnoldi's theory to include this effect.

In the Garrick and Watkins loading noise theory[2] chordwise noncompactness was included approximately by projecting the airfoil loading distribution onto a disk rather than onto a helicoid as in the present work. It turns out that the only difference this makes in the final result is to change the form of the arguments of Ψ_D and Ψ_L in Eqs. (37) and (38). That is, the Garrick and Watkins equations are obtained by setting $k_x=2mBB_D/z$. This form for k_x is correct for the

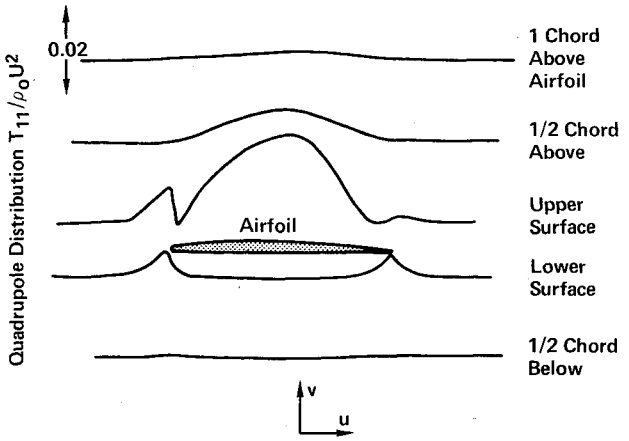

Fig. 4 Distribution of quadrupole strength around airfoil based on two-dimensional transonic flow calculations; series 16 airfoil: 3% thickness ratio, 0.15 design lift coefficient, Mach number = 0.85, angle of attack = 0, lift coefficient = 0.21.

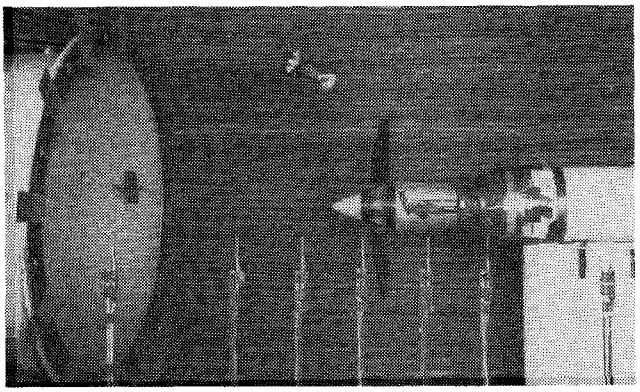

Fig. 5 Test arrangement for prop fan in UTRC acoustic wind tunnel. 7 microphones in foreground; wind tunnel nozzle at left.

static case, $M_x = 0$; however, in forward flight the Doppler factor causes an error of about 3 in k_x for prop fans at the peak radiation angle. As will be seen in Ref. 10, omitting this factor will cause a substantial overprediction in loading noise.

The Hawkings and Lowson treatment of static propeller noise[12] used essentially the same model for thickness and loading as is used here and their theory is recovered exactly from Eqs. (36-38) by setting the flight Mach number $M_x = 0$.

Finally, Hanson and Fink[11] investigated the role of quadrupole sources for the static, zero lift case. Their quadrupole noise equations are obtained by setting $M_x = 0$ for the P_{ijm} terms in Eq. (36).

Comparison with Test Results

Before exploring the theory derived above in any detail, it must be checked against test data to verify its accuracy. The most critical test of a theory is comparison of waveforms because they preserve sign and phase information whereas spectra do not. The hardware chosen for comparison is a two-bladed version of the Hamilton Standard SR-1 prop fan as tested in 1976 in the United Technologies Acoustic Wind Tunnel shown in Fig. 5. The blade characteristics are given in Fig. 6. The test was conducted at 0.32 flight Mach number and 1.049 tip helical Mach number. The spanwise distribution of lift coefficient shown in Fig. 7 was calculated from lifting-line aerodynamic theory. For loading noise predictions, the chordwise distribution of Δp was arbitrarily assumed to have a parabolic shape.

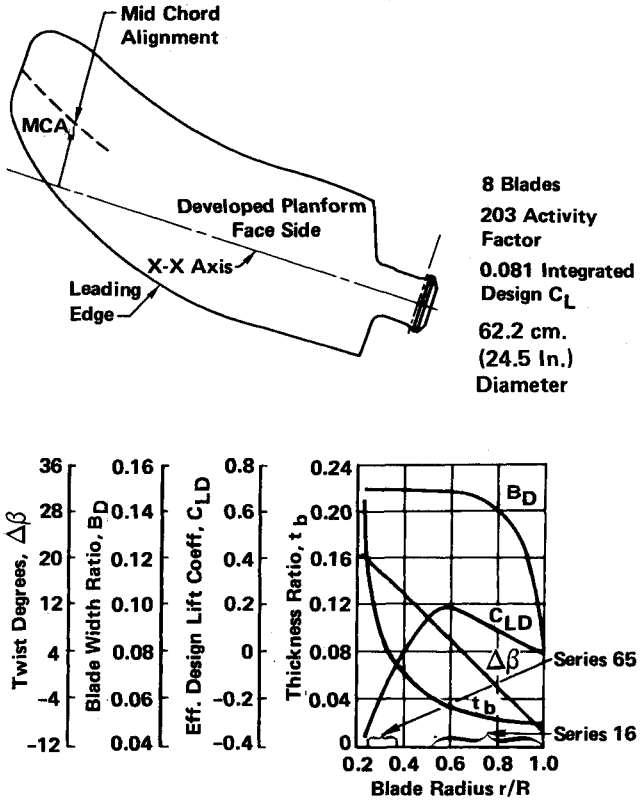

Fig. 6 Characteristics of SR-1 prop fan blade used in test data comparison.

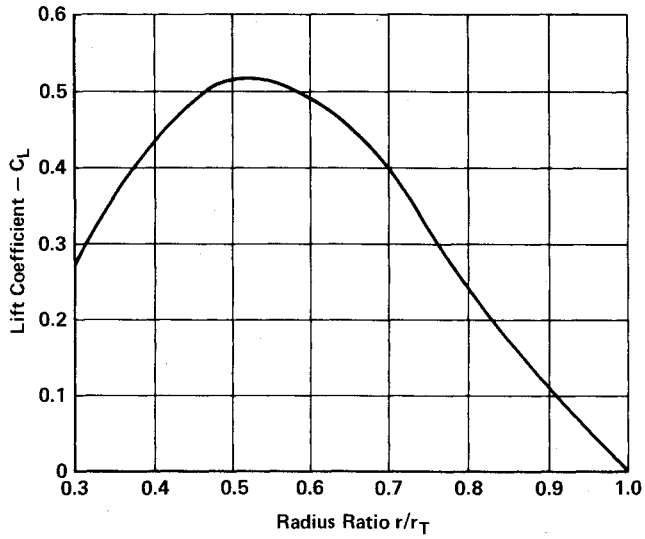

Fig. 7 Radial distribution of lift coefficient used for SR-1 prop fan noise calculations.

The comparison with data is shown in Fig. 8 where the theoretical waveforms were calculated according to

$$p(t) = \sum_{m=-80}^{80} (P_{Vm} + P_{Lm}) e^{-imB\Omega t} \tag{45}$$

where only the monopole thickness and the dipole lift components were used. (It was calculated with the P_{Dm} term of Eq. (36) that the dipole drag noise component is negligable for thin blades with reasonably good lift/drag ratios). The frequency Ω rather than the Doppler frequency Ω_D was used because there is no Doppler shift in the wind tunnel.

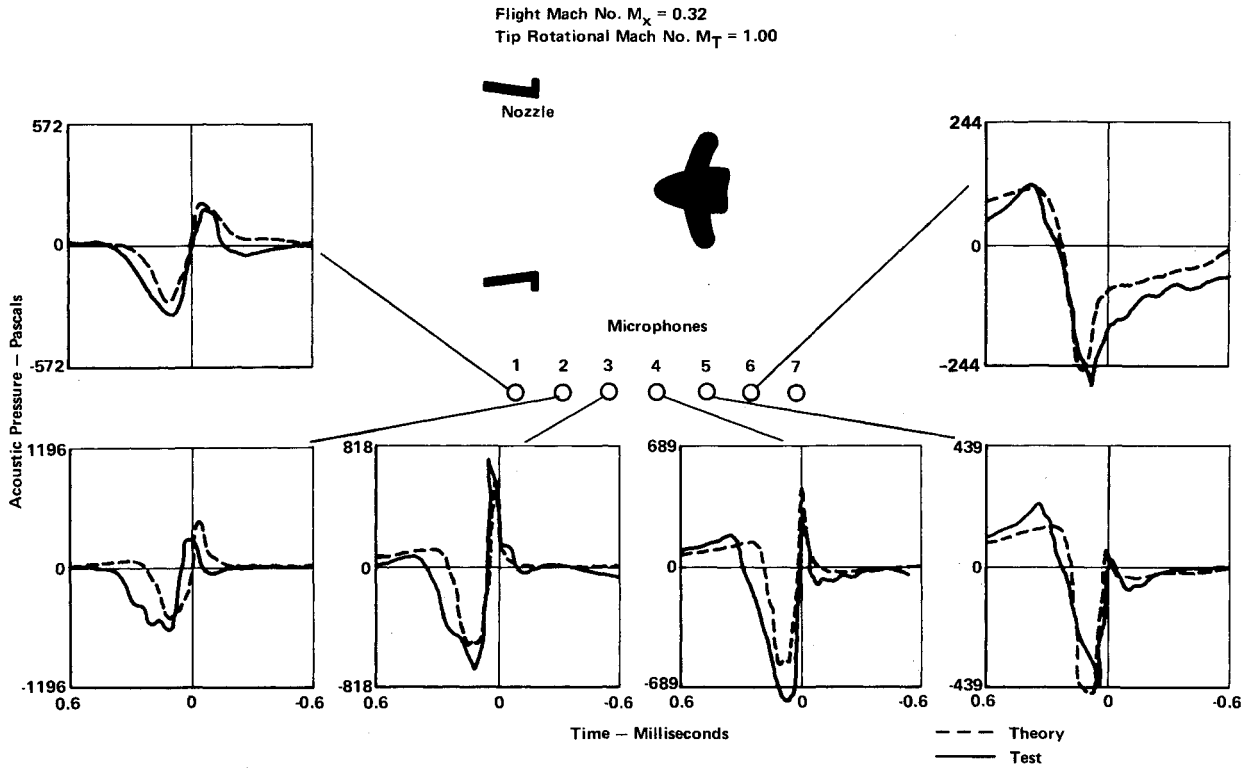

Fig. 8 Comparison of theoretical and experimental waveforms for a two-blade SR-1 prop fan tested in UTRC acoustic wind tunnel; predictions include dipole lift and monopole components only.

Figure 8 shows that the linear theory predicts experimental waveshapes and their changes with directivity satisfactorily, with the exception of small differences in pulse width and amplitude. Further comparison with test data are given in a prop fan test report.[13] Some of these results are summarized by Hanson[14] who shows for more highly swept blades (the SR-3 prop fan design shown in Fig. 1 of Ref. 10) that linear theory agrees well in all respects with test data. Evidently, with adequate sweep, the flow is linearized. Reference 14 also shows for unswept supersonic blades with subsonic-type airfoil sections that the existence of a detached bow shock explains the discrepancy between theoretical and experimental pulse widths. The fact that this flow phenomenon cannot be handled conveniently with quadrupoles is not a problem in practice because supersonic propellers would not be designed without sweep.

Conclusion

A new theoretical propeller noise formulation has been derived that refines and extends the previous frequency domain theories by distributing the blade sources on a helicoid. Many of the blade design parameters appear explicitly and in simple forms that indicate their effects on noise amplitude and phase. The linear theory is shown to agree sufficiently well with prop fan data to warrant studying in detail. This is done in another paper.[10]

Appendix: Evaluation of an Integral

The integral in question is Eq. (25), which can be rewritten:

$$I=\frac{1}{2\pi U}\int_{-\infty}^{\infty}\exp\left[-i\frac{\omega}{U}(1-M_x\cos\theta)\gamma_0\right]$$

$$\times\exp\left[i\frac{\omega r_0}{c_0}\sin\theta\cos\left(\frac{\Omega\gamma_0}{U}+\frac{V\xi_0}{Ur_0}-\pi\right)\right]d\gamma_0 \qquad (A1)$$

The second exponential can be expanded with the Bessel generating function,

$$\exp[iz\cos x]=\sum_{n=-\infty}^{\infty}J_n(z)\exp\left[in\left(x+\frac{\pi}{2}\right)\right] \qquad (A2)$$

which gives, after rearrangement,

$$I=\sum J_n\left(\frac{\omega r_0}{c_0}\sin\theta\right)\exp\left[in\left(\frac{V\xi_0}{Ur_0}+\frac{\pi}{2}\right)\right]\frac{1}{2\pi U}$$

$$\times\int\exp\left\{i\left[\frac{n\Omega}{U}-\frac{\omega}{U}(1-M_x\cos\theta)\right]\gamma_0\right\}d\gamma_0 \qquad (A3)$$

The integral can be evaluated with the Dirac delta function formula

$$\delta(\alpha)=\frac{1}{2\pi}\int_{-\infty}^{\infty}e^{i\omega\alpha}d\omega \qquad (A4)$$

to establish Eq. (26).

References

[1] Gutin, L. J., "On the Sound Field of a Rotating Propeller," translated as NACA TM 1195, 1938.

[2] Garrick, I. E. and Watkins, C. E., "A Theoretical Study of the Effects of Forward Speed on the Free-Space Sound-Pressure Around Propellers," NACA Rept. 1198, 1954.

[3] Arnoldi, R. A., "Propeller Noise Caused by Blade Thickness," United Aircraft Research Dept., East Hartford, Conn., Rept. R-0896-1, 1956.

[4] Farassat, F., "Theory of Noise Generation from Moving Helicopter Blades with an Application to Helicopter Rotors," NASA TR-R-451, Dec. 1975.

[5] Hanson, D. B., "Near Field Noise of High Speed Propellers in Forward Flight," AIAA Paper 76-565, Palo Alto, Calif., July 20-23, 1976.

[6]Schmitz, F. H. and Yu, Y. H., "Theoretical Modeling of High Speed Helicopter Impulsive Noise," *Journal of the American Helicopter Society*, Vol. 24, Jan. 1979, pp. 10-19.
[7]Goldstein, M. E., *Aeroacoustics*, McGraw-Hill Book Co., New York, 1976.
[8]Morse, P. M. and Ingard, K. U., *Theoretical Acoustics*, McGraw-Hill Book Co., New York, 1968.
[9]Carlson, L. A., "TRANDES: a Fortran Program for Transonic Airfoil Analysis or Design," NASA Rept. CR-2821, 1977.
[10]Hanson, D. B., "Influence of Propeller Design Parameters on Far-Field Harmonic Noise in Forward Flight," *AIAA Journal*, to be published.
[11]Hanson, D. B. and Fink, M. R., "The Importance of Quadrupole Sources in Prediction of High Speed Propeller Noise," *Journal of Sound and Vibration*, Vol. 62, No. 1, 1979, pp. 19-38.
[12]Hawkings, D. L. and Lowson, M. V., "Theory of Open Supersonic Rotor Noise," *Journal of Sound and Vibration*, Vol. 36, No. 1, 1974, pp. 1-20.
[13]Brooks, B. M. and Metzger, F. B., "Acoustic Test and Analysis of Three Advanced Turboprop Models," NASA CR-159667, May 1979.
[14]Hanson, D. B., "The Aeroacoustics of Advanced Turbopropellers," *Mechanics of Sound Generation in Flows*, Springer-Verlag, New York, N.Y., 1979, pp. 282-293.